IMAGE-CHARGE EFFECTS ON THE ENVELOPE DYNAMICS OF AN UNBUNCHED INTENSE CHARGED-PARTICLE BEAM

B. L. Qian, J. Zhou, and C. Chen
Plasma Science and Fusion Center, Massachusetts Institute of Technology, Cambridge, MA 02139

Abstract

The root-mean-squared (rms) envelope equations are derived and analyzed for an unbunched intense charged-particle beam in an alternating-gradient focusing field and a cylindrical conducting pipe. All higher-order image-charge effects from the cylindrical pipe are expressed in terms of so-called multiple moment factors in the rms beam envelope equations, and the multiple moment factors are evaluated. Numerical results show that for vacuum phase advance $\sigma_v < 90^\circ$, the image-charge effects on the matched and slightly mismatched beam envelopes are negligibly small, at all orders, for all beams with arbitrary beam density profiles (including hollow density profiles) as well as for arbitrary small apertures (including beams with large aspect ratios). However, the main unstable region for the envelope evolution with image-charge effects, which occurs for $90^\circ < \sigma_v < 270^\circ$, depending on the value of the normalized beam intensity SK/ε, is found to be narrower than its counterpart without image-charge effects.

INTRODUCTION

High-intensity accelerators with alternating-gradient focusing systems have many applications in basic scientific research and nuclear physics. In the research and development of high-intensity accelerators, a key issue is to minimize the aperture of the transport system for intense charge-particle beams, while preventing the beams from developing large-amplitude charge density and velocity fluctuations as well as subsequent emittance growth and halo formation. In order to understand the collective behavior of charged-particle beams, it is important to examine the beam envelope evolution under the influence of both the beam space-charge and the image charges induced on the conducting walls of accelerator structures.

The earliest works on the beam envelope equations without image-charge effects can be found in Refs. [1-4]. These works are very important for understanding the beam envelope dynamics. Recently, Lee, Close and Smith [5] and Allen and Reiser [6,7] extended Sacherer's 2-D results to include the image-charge effects due to the cylindrical conducting pipe. They analyzed the *first-order* image-charge effects.

In this paper, we extend the previous 2-D envelope equations [5-7] to include all higher-order image-charge effects from the cylindrical conducting pipe [8]. We treat the density distribution using the self-similar model, though the normal-mode analysis (i.e., small-signal theory) was used to describe the density evolution in a charged-particle beam for understanding the collective oscillations and instabilities in the beam. In particular, the self-electric and self-magnetic fields are calculated for an unbunched beam with elliptic symmetry and an arbitrary transverse dependence in the self-similar beam density model. The root-mean-squared (rms) envelope equations are derived, including all higher-order image-charge effects from the cylindrical conducting pipe. Useful numerical results on the beam envelope dynamics are presented.

BEAM ENVELOPE EQUATIONS WITH IMAGE-CHARGE EFFECTS

We consider an unbunched elliptical beam propagating in an alternating-gradient focusing field and a cylindrical metal pipe with radius R, as shown in Fig. 1. The beam has an envelope $a(s)$ in the x-direction and an envelope $b(s)$ in the y-direction, where $s = z$. The beam drift velocity in the z direction is $v_z \approx \beta_b c$, where c is the speed of light in vacuum. Following the analysis of Sacherer [3], we have derived the generalized envelope equations with image-charge effects, which can be expressed as [8]

$$\frac{d^2X}{ds^2} + \kappa_q(s)X - 2K\left[\frac{1}{X+Y} + \sum_{l=1}^{\infty} \frac{X\left(X^2 - Y^2\right)^{2l-1}}{R^{4l}} N_l\right] = \frac{\varepsilon_x^2}{X^3} \quad (1)$$

and

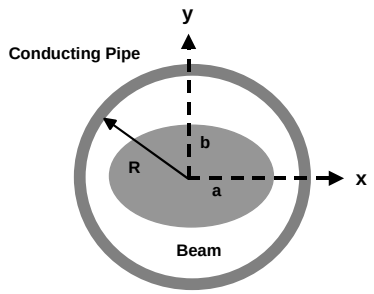

Fig. 1 Elliptical unbunched charged particle beam in a cylindrical conducting pipe.

$$\frac{d^2Y}{ds^2}-\kappa_q(s)Y-2K\left[\frac{1}{X+Y}+\sum_{l=1}^{\infty}\frac{Y\left(Y^2-X^2\right)^{2l-1}}{R^{4l}}N_l\right]=\frac{\varepsilon_y^2}{Y^3}. \quad (2)$$

In Eq. (2), $X=2\tilde{x}$ and $Y=2\tilde{y}$; $\tilde{x}=\sqrt{\langle x^2\rangle}$ and $\tilde{y}=\sqrt{\langle y^2\rangle}$ are the rms envelopes in the x- and y-directions, respectively; ε_x and ε_y are 4 times the beam rms emittances in the x- and y-directions, respectively;

$$N_l=2\left(\frac{(2l)!}{4^l(l!)^2}\right)^2\frac{\left[\int_0^{\infty}2\pi abn\left(\hat{r}^2\right)\hat{r}^{2l+1}d\hat{r}\right]^2\left[\int_0^{\infty}2n\left(\hat{r}^2\right)\hat{r}d\hat{r}\right]^{2l}}{N_b^2\left[4\int_0^{\infty}n\left(\hat{r}^2\right)\hat{r}^3d\hat{r}\right]^{2l}} \quad (3)$$

is a multiple moment factor related to the beam density profile of $n=n\left[\left(x^2/a^2\right)+\left(y^2/b^2\right)\right]$.

Unlike the previous results [5-7], which include only the $l=1$ contribution, the present envelope equations (1) and (2) are complete, including both the $l=1$ contribution and all of the higher-order image-charge effects with $l\geq 2$.

EVALUATION OF MULTIPLE MOMENT FACTORS

The multiple moment factor N_l contains the information about the higher-order image-charge effects in the envelope equations (1) and (2). We can assess these effects by evaluating N_l as a function of l. In particular, we consider the following parabolic density profile,

$$n=\begin{cases}n_0+\delta n_0\left[1-3\left(\dfrac{x^2}{a^2}+\dfrac{y^2}{b^2}\right)^2\right], & \dfrac{x^2}{a^2}+\dfrac{y^2}{b^2}\leq 1,\\ 0, & \dfrac{x^2}{a^2}+\dfrac{y^2}{b^2}>1,\end{cases} \quad (4)$$

where $N_b=\int_{-\infty}^{\infty}\int_{-\infty}^{\infty}n\,dxdy=\pi abn_0=\text{constant}$ and δn_0 is independent of x and y and satisfies $-n_0\leq\delta n_0\leq n_0/2$.

Using Eq. (4) and the moment definition, we can obtain the simplified expressions of envelopes X and Y. They are written in the form of $X^2=a^2(1-g/2)$ and $Y^2=b^2(1-g/2)$. In addition, substituting Eq. (4) into Eq. (3), we obtain

$$N_l=2\left(\frac{(2l)!}{4^l(l!)^2}\right)^2\left(\frac{1}{1-0.5g}\right)^{2l}\left(\frac{1-2gl/(l+3)}{l+1}\right)^2 \quad (5)$$

where $g=\delta n_0/n_0$. Note in Eq. (5) that $N_1=1/8=0.125$ is independent of the factor g. Figure 2 shows a plot of N_l as a function of l for three cases corresponding to $g=0$, 0.5, and -0.5.

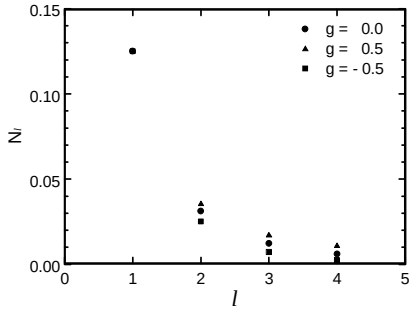

Fig. 2 The dimensionless multiple moment factor N_l versus l for several densities with $g=0$, 0.5, and –0.5.

IMAGE-CHARGE EFFECTS ON RMS MATCHED BEAMS

In this section, we show that for vacuum phase advance $\sigma_v<90^\circ$, the higher-order image-charge effects on the matched beam envelopes are negligibly small for all beams with arbitrary beam density profiles (including hollow density profiles) as well as for arbitrary small apertures (including beams with large aspect ratios). We pay special attention to a hollow beam observed in a recent heavy ion beam experiment.

For present purposes, we assume that the rms emittances ε_x and ε_y are constant, i.e., $\varepsilon_x=\varepsilon_y=\varepsilon$, and that the beam density profile is given in Eq. (4). We also assume that the alternating-gradient transport system is presented a step-function lattice defined by [9]

$$\kappa_q(s)=\begin{cases}+\kappa_{q0}, & 0\leq s/S<0.25\eta,\\ 0, & 0.25\eta\leq s/S<0.5(1-0.5\eta),\\ -\kappa_{q0}, & 0.5(1-0.5\eta)\leq s/S<0.5(1+0.5\eta),\\ 0, & 0.5(1+0.5\eta)\leq s/S<0.5(2-0.5\eta),\\ +\kappa_{q0}, & 0.5(2-0.5\eta)\leq s/S<1,\end{cases} \quad (6)$$

where κ_{q0} is a constant and η $(0<\eta<1)$ is the filling factor.

In the numerical analysis of the beam envelope equations (1) and (2), it is convenient to use the dimensionless parameters and normalized variables defined by $\hat{s}=s/S$, $\tilde{a}=X/\sqrt{S\varepsilon}$, $\tilde{b}=Y/\sqrt{S\varepsilon}$, $\hat{K}=KS/\varepsilon$, $\hat{R}=R/\sqrt{S\varepsilon}$, and $\tilde{\kappa}_q(s)=S^2\kappa_q(s)$. For example, Fig. 3 shows the matched beam envelope functions for beam propagation in free space as well as in a cylindrical conducting pipe. It is evident in Fig. 3 that the image-charge effects, including the contributions from all orders, are negligibly small for a hollow beam whose maximum

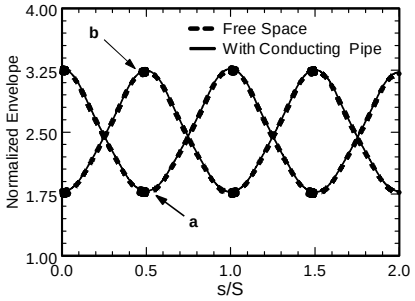

Fig. 3 Plot of the normalized envelope functions $\tilde{a}$ and $\tilde{b}$ versus normalized propagating distance s/S for vacu phase advance $\sigma_v = 80^0$, $\hat{K} = 10$, $g = -0.5$, $\eta = 0.5$, and $\hat{R} = 4.0$.

envelopes are very close to the wall of the cylindrical pipe ($\tilde{a}_{\max} = \tilde{b}_{\max} \approx 3.25$ and $\hat{R} = 4.0$).

IMAGE-CHARGE EFFECTS ON SLIGHTLY MISMATCHED BEAMS AND ENVELOPE INSTABILITIES

In a real device, it is almost impossible to obtain a precisely matched beam because there are some perturbations on the beam propagation. These perturbations may cause beam envelope instabilities, and the unstable beam envelopes may result in particle beam losses. The beam envelope instability has already been investigated in free space [9]. However, the image-charge effects of the cylindrical conducting pipe on the mismatched beams and the beam envelope instability have not been studied until the present paper. In this section, the envelope equations (1) and (2) are solved, assuming $\varepsilon_x = \varepsilon_y = \varepsilon$, for slightly mismatched beams to find the unstable regions in the parameter space.

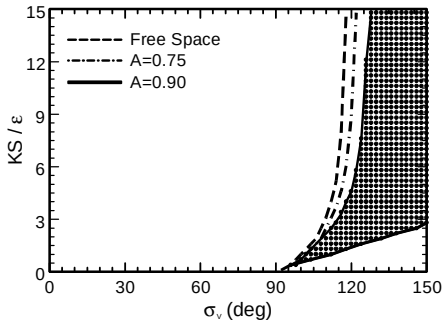

Fig. 4 Plot of the unstable regions in the dimensionless parameter space for the beam envelope evolution with $\eta = 0.5$ and $g = 0$ for three cases corresponding to (a) $R = \infty$ (free space), (b) $A = \tilde{a}_0 / \hat{R} = 0.75$, and (c) $A = \tilde{a}_0 / \hat{R} = 0.90$. Here, the shaded region is the unstable region for the beam envelope evolution with image-charge effects and $A = \tilde{a}_0 / \hat{R} = 0.90$.

In order to obtain slightly mismatched beam envelopes, following the method employed in Ref. [9], the initial conditions for $\tilde{a}(s)$ and $\tilde{b}(s)$ at $s = 0$ are chosen to be $\tilde{a}(0) = \tilde{a}_0(1+\delta)$ and $\tilde{b}(0) = \tilde{b}_0(1-\delta)$, where $\tilde{a}_0$ and $\tilde{b}_0$ are the matched beam envelopes at $s = 0$ and δ is chosen to be in the region of $0 \le |\delta| \le 0.01$. Here, δ represents the perturbations caused by the noise in the beam. In the numerical calculations, the particle beams are allowed to propagate over 40 periods.

Figure 4 is a plot of $\hat{K} = KS/\varepsilon$ versus σ_v, showing the unstable regions of the slightly mismatched beam envelopes. As can be seen from Fig. 5, the unstable regions for all the three cases start around $\sigma_v = 90°$. The solid lines indicate the boundary of the unstable region with image-charge effects from the cylindrical pipe for $A = \tilde{a}_0 / \hat{R} = 0.90$, whereas the dashed lines represent the boundary of unstable region without image-charge effects in free space. The unstable region with image-charge effects for $A = \tilde{a}_0 / \hat{R} = 0.90$ is shaded in Fig. 4. Although the lower boundaries for the three cases almost coincide, there is an observable difference between their upper boundaries. The unstable region for cylindrical pipe case (i.e., with image-charge effects) is obviously narrower than that in free space situation (i.e., without image-charge effects).

This research was supported by the U. S. Department of Energy, Division of High-Energy Physics, Grant No. DE-FG02-95ER40919, and Office of Fusion Energy Science, Grant No. DE-FG02-01ER54662.

REFERENCES

[1] I. M. Kapchinskij and V. V. Vladimirskij, in *Proceedings of the International Conference on High Energy Accelerators and Instrumentation* (CERN, Geneva, 1959), p. 274.
[2] P. Lapostolle, CERN Report AR/Int. SG/65-15 , (1965).
[3] F. J. Sacherer, IEEE Trans. Nuclear Sci. **NS-18**, 1105 (1971).
[4] P. Lapostalle, IEEE Trans. Nuclear Sci. **NS-18**, 1101 (1971).
[5] E. P. Lee, E. Close, and L. Smith, in *Proceedings of the 1987 IEEE Particle Accelerator Conference*, edited by E. R. Lindstorm and L. S. Taylor (Institute for Electrical and Electronic Engineers, New York, 1987), p. 1126.
[6] C. K. Allen and M. Reiser, Phys. Rev. **E 54**, 2884(1996).
[7] C. K. Allen, Ph. D. dissertation, University of Maryland, (1996).
[8] B. L. Qian, J. Zhou, and C. Chen, Phys. Rev. ST-AB **6**, 014201(2003).
[9] Q. Qian and R. C. Davidson, Phys. Rev. **E53**, 5349 (1996).